JOURNAL OF MORPHOLOGY 276:301–309 (2015)

The Shrew Tamed by Wolff's Law: Do Functional Constraints Shape the Skull Through Muscle and Bone Covariation?

Raphaël Cornette,[1]* Anne Tresset,[2] and Anthony Herrel[3,4]

[1]*UMR CNRS/MNHN/UPMC/EPHE 7205, "Institut de Systématique, Évolution et Biodiversité," Muséum National d'Histoire Naturelle, 45 Rue Buffon, 75005 Paris, France*
[2]*UMR CNRS/MNHN 7209, "Archéozoologie, Archéobotanique: Sociétés, Pratiques et Environnements," Muséum National d'Histoire Naturelle, 55 Rue Buffon, Case Postale 56, 75005 Paris, France*
[3]*UMR CNRS/MNHN 7179, "Mécanismes Adaptatifs: Des organismes Aux Communautés," Muséum National d'Histoire Naturelle, 57 Rue Cuvier, 75231 Paris Cedex 05, France*
[4]*Evolutionary Morphology of Vertebrates, Ghent University, K.L. Ledeganckstraat 35, B-9000 Gent, Belgium*

ABSTRACT Bone is a highly plastic tissue that reflects the many potential sources of variation in shape. Here, we focus on the functional aspects of bone remodeling. We choose the skull for our analyses because it is a highly integrated system that plays a fundamental role in feeding and is thus, likely under strong natural selection. Its principal mechanical components are the bones and muscles that jointly produce bite force and jaw motion. Understanding the covariations among these three components is of interest to understand the processes driving the evolution of the feeding apparatus. In this study, we quantitatively and qualitatively compare interactions between these three components in shrews from populations known to differ in shape and bite force. Bite force was measured in the field using a force transducer and skull shape was quantified using surface geometric morphometric approaches based on μCT-scans of the skulls of same individuals. The masseter, temporalis, pterygoideus, and digastricus muscles of these individuals were dissected and their cross sectional areas determined. Our results show strong correlations between bite force and muscle cross sectional areas as well as between bite force and skull shape. Moreover, bite force explains an important amount of skull shape variation. We conclude that interactions between bone shape and muscle characteristics can produce different morpho-functional patterns that may differ between populations and may provide a suitable target for selection to act upon. J. Morphol. 276:301–309, 2015.

KEY WORDS: mammals; 3D-geometric morphometrics; bite force; feeding apparatus

INTRODUCTION

Wolff's law, in its most general sense, stipulates that functional constraints shape bones (Wolff, 1892). Indeed, bone is a plastic material, constantly remodeling when submitted to mechanical constraints (Currey, 2002, 2003; Sharir et al., 2011; Slizewski et al., 2013). The fact that bone remodels in response to mechanical loading has direct consequences on the evolution of bone shape (Weijs and Hillen, 1986; Hannam and Wood, 1989; Raadsheer et al., 1999; Mavropoulos et al., 2004). Even if the shape of a bone results from numerous and complex processes including developmental constraints, environmental plasticity and phylogeny, functional constraints are thought to drive an important part of bone shape as bone directly responds and remodels in response to both muscle and external forces (Currey, 2002). Given that the association between form and function (i.e., the morpho-functional pattern) is a likely target of natural selection, understanding these relationships is important.

The skull is a high integrated system with numerous associated functions including, among others, olfaction, vision, protection of the brain, as well as feeding (Wake and Roth, 1989; Hanken and Hall, 1993). During feeding the generation of bite force is of principal importance as it is related to the ability to capture, kill, and reduce a food item (Anderson et al., 2008). During feeding jaw

Additional Supporting Information may be found in the online version of this article.

Contract grant sponsor: M.N.H.N./A.T.M. (Formes possibles, Formes réalisées); Contract grant sponsor: M.N.H.N./A.T.M. (Biodiversité actuelle et fossile).

*Correspondence to: Raphaël Cornette, UMR CNRS/MNHN/UPMC/EPHE 7205, "Institut de Systématique, Évolution et Biodiversité," Muséum National d'Histoire Naturelle, 45 Rue Buffon, 75005 Paris, France. E-mail: cornette@mnhn.fr

Received 1 July 2014; Revised 8 October 2014; Accepted 26 October 2014.

Published online 11 November 2014 in Wiley Online Library (wileyonlinelibrary.com). DOI 10.1002/jmor.20339

movements are modulated through the action of four principal muscle groups in mammals: the masseter, the temporalis, and the pterygoidus that function to close the jaw and the digastricus being the jaw opener (Turnbull, 1970). Through the differential activation of these muscles, bite force is modulated allowing for an extensive intraoral processing of the food in mammals (Ross et al., 2007). Whereas selection undoubtedly acts on the efficiency of jaw movements in mammals (Ross et al., 2010), maximal bite force generation capacity is likely also under selection as it determines the maximal size or hardness of a food item that can be eaten (Aguirre et al., 2003).

Previous studies have shown clear relationships between cranial shape and bite force, especially in shrews (Young et al., 2009; Cornette et al., 2012, 2013). Shrews are small insectivorous mammals that are known to eat a wide variety of prey (Churchfield, 1990), including significant amounts of hard-bodied arthropod prey (Young et al., 2009). Moreover, shrews possess a late ossification of the mandible suggesting that they may be impacted more markedly than other small mammals by plastic remodeling of the jaws (Young and Badyaev, 2010). Indeed, the morpho-functional patterns established during development may be modified more easily in shrews given that juveniles capture and reduce prey before the complete ossification of the mandible (Young and Badyaev, 2010). As a result of this plasticity, different populations have specific shape patterns of the skull and mandible based on the local availability of prey (Young et al., 2009; Cornette et al., 2013). This is most clearly exemplified in the shape differences observed between insular and continental populations with continental populations having an enlarged posterior portion of the skull and well developed coronoid and angular processes.

Here, we explore the morpho-functional patterns in the skull of the greater white-toothed shrew by comparing how bite force and muscle physiological cross sectional area (PCSA) affect shape evolution in this species. Specifically, we aim to investigate (I) the relationships between skull shape and in vivo bite force; (II) the relationships between variation in muscle cross sectional area and skull shape; and (III) the differences in shape variation between shrews from islands and continental individuals. To do so, we use 3D-geometric morphometric approaches based on μCT-scans for individuals from both, islands and continental France. Moreover, muscle cross sectional area data and in vivo bite forces are collected for these same individuals. We predict that the animals from the island will be characterized by a cranial shape that is similar to that observed in individuals with low bite forces given previous suggestions of low bite force in insular shrew populations (Cornette et al., 2012). Moreover, we specifically predict that specimens with high bite force and those with large temporalis muscles will show an enlarged parietal area of the skull, the insertion site for the temporalis muscle. Additionally, we predict that these specimens will also have shorter rostra, thus, decreasing the outlever of the jaw system and increasing bite force at the incisors for a given muscle cross sectional area.

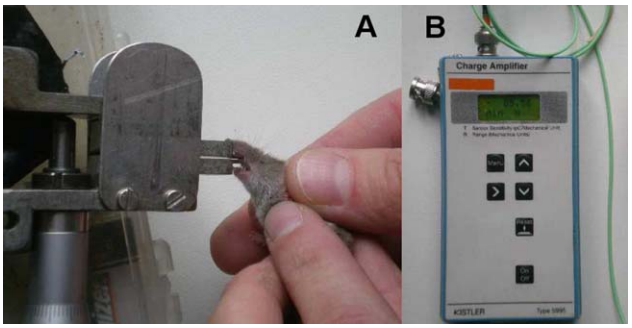

Fig. 1. Set-up used to measure bite forces. Animals were induced to bite two metal plates (**A**) holding an isometric force transducer and connected to (**B**) a portable charge amplifier. [Color figure can be viewed in the online issue, which is available at wileyonlinelibrary.com.]

MATERIALS AND METHODS

Specimens

Greater white-toothed shrews, *Crocidura russula* (Hermann, 1780) from island and continental populations were used for this study. Island populations are known to be different in shape and estimated bite force from continental populations (Young and Badyaev, 2010; Cornette et al., 2012, Cornette et al., 2013). Here, we base our analysis on four continental specimens, three from Souppes sur Loing (Seine et Marne, France), and one from Mer (Loir et Cher, France), as well as three specimens from Belle-Île island (Morbihan, France). Adult specimens were trapped and bite force was measured using an isometric Kistler force transducer (Kistler, type 9203, range ±500 N; Kistler, Winterthur, Switzerland; see Herrel et al., 1999; Aguirre et al., 2002; Fig. 1). At least three recording sessions were performed, each of which including at least five bites. The highest bite force measured was retained and considered the maximal bite force of an individual (Chazeau et al., 2013). After measurements were taken, animals were euthanized in accordance with animal care and use protocols (lethal injection of pentobarbital). All experiments were approved by the animal care and use committee at the MNHN.

Dissections

Specimens were preserved in 10% formaldehyde solution for 48 h, rinsed and transferred to a 70% ethanol solution. All muscles linking the lower jaw with the cranium (i.e., the masseter, the temporalis, the pterygoideus, and the digastric) were dissected and muscle bundles were removed individually and preserved in 70% ethanol (Herrel et al., 2008; see Fig. 2). Muscles were blotted dry and weighed using a Mettler AE100 electronic balance (±0.0001 g). Next, muscles were transferred to a 30% nitric acid solution for 24–48 h until the connective tissue surrounding the muscle fibers was dissolved (Loeb and Gans, 1986). Once fibers could be teased apart using blunt-tipped glass needles the nitric acid was removed and replaced by a 50% aqueous glycerol solution. Ten to twenty fibers were drawn using a stereomicroscope with *camera lucida* and a

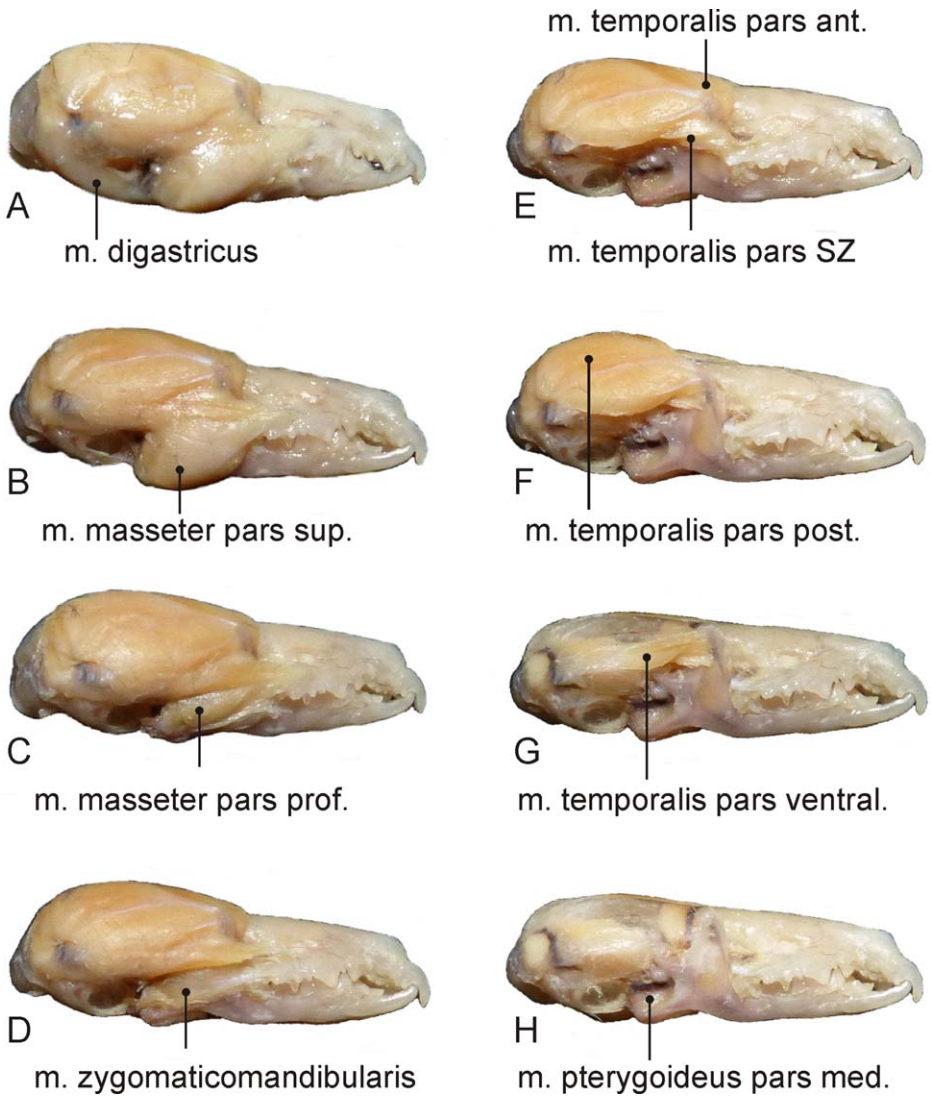

Fig. 2. *Crocidura russula* different jaw adductor muscles. (**A**) Superficial right lateral view after removal of the skin. (**B**) After removal of the m. digastricus. (**C**) After removal of the m. masseter pars superficialis. (**D**) After removal of the m. masseter pars profundus. (**E**) After removal of the m. zygomaticomandibularis. (**F**) After removal of the m. temporalis pars suprazygomatica (SZ) and pars anterior. (**G**) After removal of the m. tempralis pars posterior. (**H**) After removal of the m. temporalis pars ventralis. [Color figure can be viewed in the online issue, which is available at wileyonlinelibrary.com.]

known scale for each muscle bundle. Drawings were scanned and fiber lengths measured using image J. The volume of each muscle bundle was then calculated by dividing muscle mass by muscle density (1.06 g cm^{-3}; Mendez and Keys, 1960) and PCSA was calculated by dividing the volume by fiber length.

Cross sectional areas of the different muscle bundles were then summed to calculate the cross sectional area of each major muscle group. To quantify effects of different muscles while maintaining a multivariate approach, a principal component analysis (PCA) on variance-covariance matrix was performed on the muscle data from the different individuals. The first two axes, together explaining nearly 90% of the overall variation among individuals, were extracted.

3D-Morphometrics

All specimens were scanned at a resolution of 30 μm using an XRA-002 micro-CT scan (X-Tek, Tyngsboro, MA) available at the Center for Nanoscale System at Harvard University. Scans were segmented using AVIZO (VSG, Burlington, MA). To accurately describe variation in skull shape, we followed the procedures detailed in Cornette et al. (2013): first, we recorded the 3D-coordinates of anatomical landmarks and curves in the program Landmark (Wiley et al., 2005; Fig. 3). Next, we used the template developed by Cornette et al. (2013) identifying surface landmarks needed to quantify the overall skull shape (Fig. 3). The template was first prepositioned based on the true landmarks and then landmarks were projected onto the surface of the specimen to be measured. Next, sliding of the landmarks on the surface was performed while minimizing the bending energy between the template and the specimen (Gunz and Mitteroecker, 2013). All these procedures were performed using edgewarp (Bookstein and Green, 2002). Finally, we exported landmark coordinates and imported them in R (R Development Core Team, 2013) to perform geometric morphometric and statistical analyses using the libraries "Rmorph" (Baylac, 2012) and "Ape" (Paradis, 2012).

We performed a general procrustes analysis (Rohlf and Slice, 1990) followed by a PCA on the Procrustes residuals.

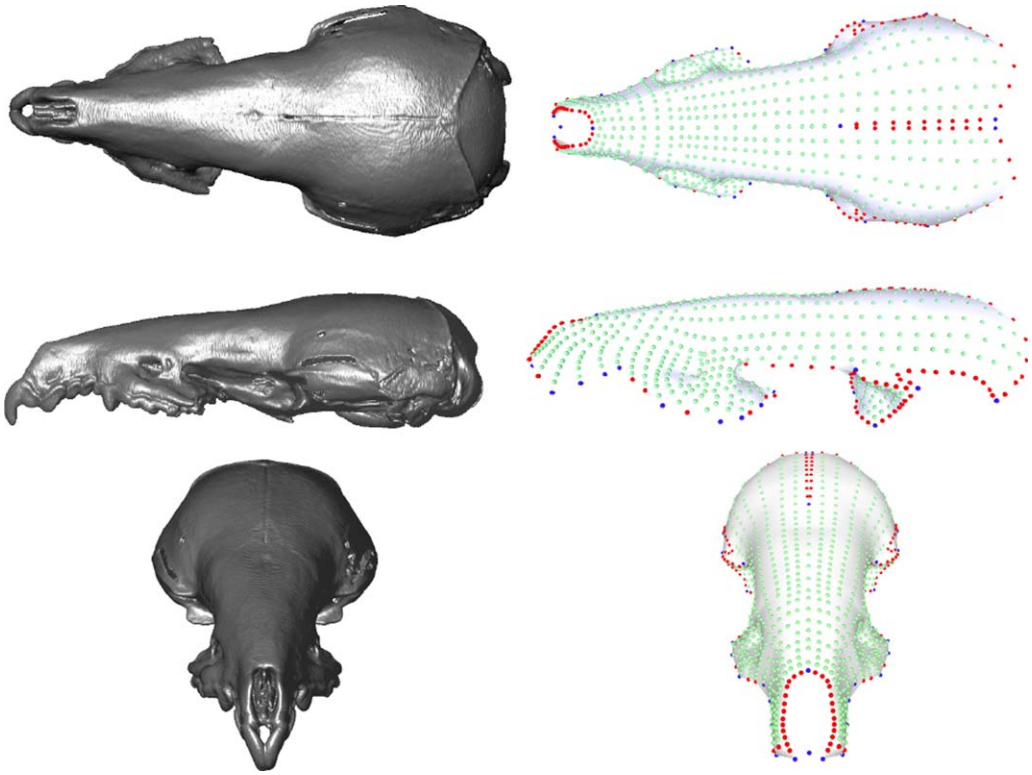

Fig. 3. *Crocidura russula*, original μCT-scans (left) and the template built to describe skull shape (right) in dorsal, lateral, and oblique frontal view. Blue landmarks represent anatomical landmarks, red ones represent landmarks on curves, and green ones represent the sliding surface landmarks (see Cornette et al., 2013).

Multivariate regressions (Monteiro, 1999) were then used to visualize the effect of variation in muscle data or bite force on cranial shape in R using the RMorph-library (Baylac, 2012). These 3D-visualizations were performed using MeshLab (Visual Computing Lab -ISTI-CNR, http://meshlab.source.forge/) and Avizo (VSG, Burlington, MA) as described previously (Cornette et al., 2013). This allows the visualization of cranial shape (magnitude, location, and direction) along the three principal axes of shape variation (i.e., the first three PCA's). In addition, it allows the visualization of the effects of size, bite force (BF), bite force corrected by centroid size (BFht), and muscle PCSAs (muscle by muscle or summarized by a PCA performed on the data). Finally, we visualized shape variation among individuals from the island versus continental populations. To compare these shapes, a neighbor joining tree was created using the Euclidean distances between all shape configurations.

RESULTS

Muscles

The jaw musculature in shrews diverges from the general mammalian type due to the absence of the zygomatic arch. The temporalis muscle is the largest of all the jaw adductors (Table 1) and runs from its origin on the brain case to the well developed coronoid process of the lower jaw (Fearnhead et al., 1954; Gasc, 1963; Dötsch, 1986; Fig. 2). The temporalis can be subdivided in three major muscle bundles as described in Dötsch (1986). Whereas, the ventral most and posterior parts have a mostly horizontal line of action, the anterior part has more vertically directed muscle fibers. The masseter is highly divergent from the typical mammalian situation due to the absence of the zygomatic arch. The superficial part is the largest part of the masseter and runs from its tendinous origin on the maxilla to its tendinous insertion on the distal lateral aspect of the angular. The deeper fibers have a fleshy origin on the posterior aspect of the maxilla and have a fleshy insertion on the lateral aspect of the angular process. The deepest bundle, possibly homologous to the zygomaticomandibularis in other mammals originates tendinously from the posterior, most part of the maxilla and has a fleshy insertion on the dorsolateral aspect of the angular process. The pterygoideus is subdivided into two parts, a more superficial lateral part with a medio-lateral orientation, and a deeper part with a more anterio-posterior line of action (Dötsch, 1986). Finally, the single jaw opener, the digastricus muscle originates from the paraoccipital process and inserts tendinously on the ventral side of the mandibular ramus.

A PCA performed on the muscle PCSAs extracted two axes, together explaining nearly 90% of the overall variation in the dataset (Fig. 4). Whereas, the second axis correlated negatively with the cross sectional area of the temporalis, yet

TABLE 1. Raw muscle and bite force data used in the analyses

Origin	Digastricus (cm^2)	Temporalis (cm^2)	Masseter (cm^2)	Pterygoideus (cm^2)	Bite force (N)
Belle Isle	0.020	0.120	0.049	0.029	4.64
Belle Isle	0.013	0.125	0.044	0.024	4.29
Belle Isle	0.015	0.122	0.036	0.033	4.29
Belle Isle	0.024	0.123	0.073	0.019	4.58
Souppes	0.023	0.159	0.086	0.027	5.69
Souppes	0.024	0.185	0.083	0.052	6.49
Souppes	0.024	0.149	0.084	0.041	5.87
Mer	0.017	0.133	0.050	0.034	4.98

positively with that of the other muscles; the first axis correlated positively with the temporalis and pretygoideus muscles, yet negatively with the masseter and the digastricus. This analysis suggests that the specimens from Belle Isle island have lower temporalis cross sectional areas but relatively well developed masseter and digastricus muscles compared to specimens from the continent (Fig. 4).

Shape Differences

The first principal component highlights shape differences (34.87% of the total shape variation; Supporting Information Fig. S1a) mainly situated at the lower part of the rostrum and the upper posterior part of the skull. Important shape differences are also situated at the level of the glenoid fossae. The second principal component (27.11% of the total shape variation; Supporting Information Fig. S1b) is associated with marked differences of the middle part of the skull at the level of the frontal bones, extending to the lower part of the parietal bones. The third principal component (12.97% of the total shape variation; Supporting Information Fig. S1c) is associated with shape differences mainly situated in the molar alveolar part, the upper part of the parietal bones, and the upper part of the rostrum. When comparing the shape of insular and continental specimens, the main difference is situated in the lateral middle part of the skull at the level of the frontal bones. There are also slight differences in the shape of the upper part of the rostrum. Shape variation associated with the allometric component is situated at the middle part of the skull and extends to the lower part of the parietal bones, the alveolar dental part, the back and the lower part of the parietal bones, and the glenoid fossae (Supporting Information Fig. S2).

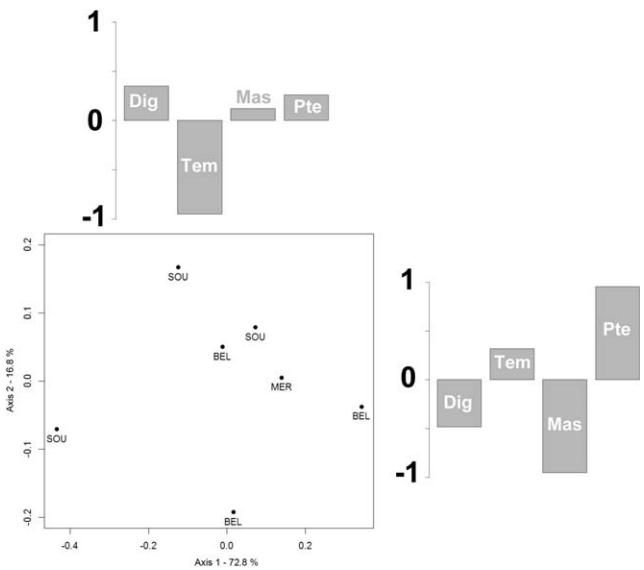

Fig. 4. Results of a PCA performed on the muscle cross sectional area data explaining almost 90% of the overall variation in the dataset. Individuals from the different populations are indicated by their locality of capture (BEL, Belle Isle; SOU, Souppes sur Loing; MER, Mer). The loadings of the different muscles cross sectional areas on axis one (to the right PC plot) and two (above of the PC plot) are indicated as well. Whereas, the first axis differentiates specimens with relatively large temporalis muscles on the negative side of the axis, the second axis contrasts specimens with large masseter muscles to specimens with large pterygoideus muscles.

Global Shape Affinities

The neighbor joining tree describing global shape affinities allows us to compare all the patterns described above (Fig. 5). Beginning along the right side of the tree, it can be noted that the shape associated with negative part of the first axis of shape variation in the sample (ACP shape A1−) is similar to the shape of specimens having high relative bite forces (BF ht+). This impacts mostly the frontal bones, the posterior most part of the skull, and the upper part of the rostrum. The shapes described by the negative part of the third shape axis (ACP shape A3−) are similar to shapes defined by the negative part of the first axis of the PCA performed on the muscular (ACP mus A1−) data and concerns the molar alveolar part, the upper part of the parietal bones, and the upper part of the rostrum. As could be expected, shape variation due to a high absolute bite force (BF+) is similar to that defined by a large temporalis (TEMP+) and pterygoideus (PTE+) cross sectional area, again principally affecting the frontal bones, the posterior most part of the skull, and the upper part of the rostrum. The shape associated with high allometry (ALLOM+) is similar to the shape represented by the negative part of the second axis describing overall shape variation in the dataset (ACP shape A2−) and the shape associated with the positive part of the second PCA axis of the analysis performed on muscular data

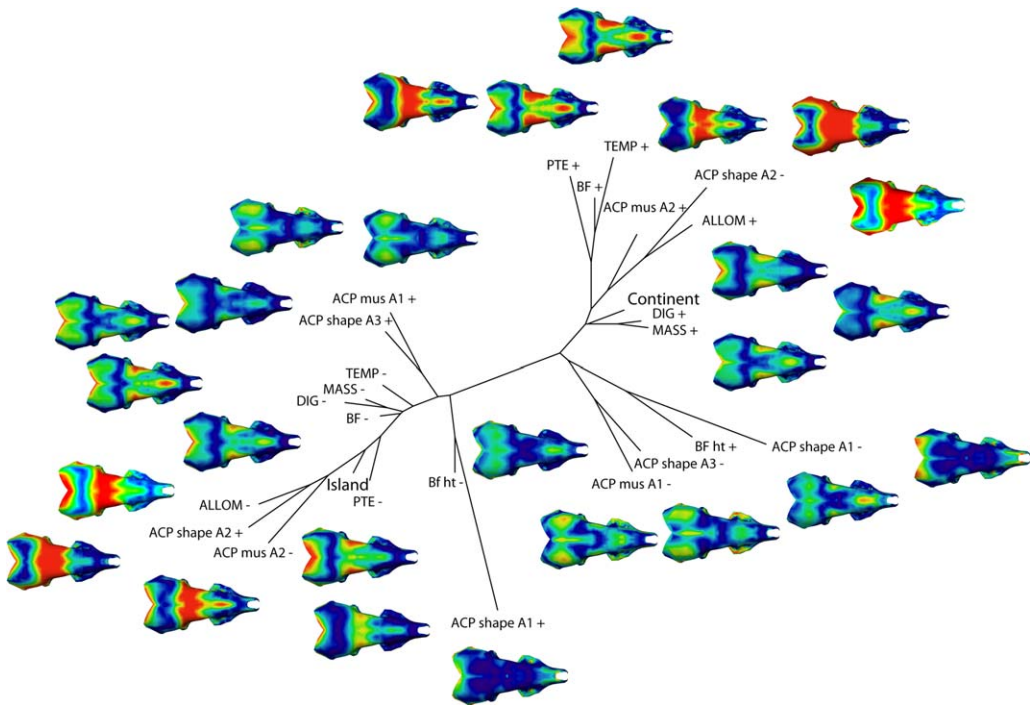

Fig. 5. Neighbor joining tree illustrating the similarity in shape associated with variation in muscle PCSA, allometry, bite force, and ecological factors (island vs. continental populations) as well as the principal axes of shape variation. Hotter colors indicate areas that show greater shape changes. For example, shape changes associated with high bite forces illustrated at the top of the tree are very similar (i.e., short branches) to those observed for large temporalis muscle cross sectional areas. Moreover, the shapes of continental specimens are similar to those of specimens with large masseter and digastrics muscle cross sectional areas as illustrated to the right of the tree. See also Supporting Information Figures S1–S5 for alternative visualizations of the overall shape change or the shapes associated with variation in muscle PCSA, bite force or allometry. + indicates either the positive side of a principal component axis or a high PCSA, bite force, or allometry; − indicates either the negative side of a principal component axis or a low PCSA, bite force, or allometry. A, axis; ACP mus, results of the PCA performed on the muscle data; ACP shape, results of the PCA performed on the shape data; ALLOM, allometry; BF, absolute bite force; BF ht, size corrected bite force; DIG, m. digastricus; MASS, m. masseter; PTE, m. pterygoideus; TEMP, m. temporalis.

(ACP mus A2+). The associated variation in shape is situated in the middle part of the skull and extends to the lower part of the parietal bones, the alveolar dental part, the back and the lower part of the parietal bones, and the glenoid fossae. Finally, the shapes associated with a large digastricus (DIG+) and masseter (MASS+) physiological cross sectional area are similar to shapes of continental specimens (Continent). Although the left part of the tree is largely a mirror image of the right part, some subtle differences should be noted: shapes associated with low absolute bite force (BF−) are similar to shapes defined by a low temporalis (TEMP−), digastricus (DIG−), and masseter (MASS−) PCSAs. Moreover, this side of the tree shows that the shape of insular specimens (Island) is similar to that of individuals with a low pterygoideus cross sectional area (PTE−).

Shape Versus Bite Force

Shape variation associated with variation in bite force reveals marked differences on three different locations: the two frontal bones, the posterior most part of the skull, and the upper part of the rostrum (Supporting Information Fig. S3a and Fig. 5). Shape differences associated with bite force corrected for variation in overall size (i.e., centroid size) are globally situated on the same parts of the skull, but a decrease in the magnitude of the shape variation can be observed (Supporting Information Fig. S3b and Fig. 5). Moreover, slight differences at the level of the glenoid fossa and the parietal bones can be observed compared to shape variation related to absolute bite force variation.

Shape Versus Muscles

Shape variation associated with the first axis of the muscle PCA is mainly situated at the level of the parietal part of the skull, the upper part of the rostrum, the molar and incisor alveolar regions, and the lateral part of the middle of the skull (Supporting Information Fig. S4a and Fig. 5). Shape variation associated with the second axis highlights marked differences in the middle part of the skull and in the upper part of the rostrum. Variation in shape is also present at the posterior most part of the parietal bones (Supporting Information Fig. S4b and Fig. 5). Shape differences associated with variation in the digastricus muscle (Supporting Information Fig. S5a and Fig. 5) are

mainly situated on the lateral part of the frontal bones and on the upper part of the rostrum. Differences also exist at the junction of the parietal bones. Shape differences associated with the masseter muscle (Supporting Information Fig. S5b and Fig. 5) are mainly situated at the level of the parietal bones, on the lateral part of the frontal zone, and on the upper part of the rostrum. Others differences are found in the molar and incisor alveolar regions, and the upper parietal junction. Shape differences associated with variation in the temporalis muscle (Supporting Information Fig. S5c and Fig. 5) are similar to those observed for variation in absolute bite force. The pterygoideus muscle (Supporting Information Fig. S5d and Fig. 5) is responsible for shape variation that is mostly situated at the middle part of the skull and the upper part of the rostrum. Variation also exists in the glenoid fossae, the molar and incisor alveolar regions, and the upper parietal junction in animals with a large versus small cross sectional area of the pterygoideus muscle.

DISCUSSION

Shape and Muscles

The first axis of the PCA performed on the cross sectional areas of the four masticatory muscles shows a pattern of variation similar to that given by the third shape axis describing overall shape variation in the dataset. The second principal component axis from the analysis on the muscle cross sectional areas illustrates a pattern of variation similar to that represented by the first principal component axis describing overall shape variation. This result highlights that variation in muscle PCSA explains a large amount of intrinsic shape variation in the dataset and thus among natural populations. Muscles not only need space for their insertions onto the cranium, they may also modify the shape of the bones they are inserting upon due to the forces they exert. As such, the relationships between quantitative descriptors of the muscle such as the PCSA and overall bone shape are likely tight as is demonstrated by our analysis. Given that selection of functional traits such as bite force is likely great, this may have cascading effects on the muscles and through the muscles also on the bones of the skull, thus, providing for integrated morpho-functional patterns on which selection can act.

Shape and BF

Relationships between variation in skull shape and bite force are well known and numerous examples exist among vertebrates: fish (Huber et al., 2009), lizards (Herrel et al., 2001, Herrel and Holanova, 2008), birds (Herrel et al., 2005), rodents (Van Daele et al., 2009) bats (Aguirre et al., 2002), or insectivores (Young and Badyaev, 2010; Cornette et al., 2013). Although bite force is often estimated using models (Young et al., 2009; Cornette et al., 2012, 2013) it can also be measured in live animals. In vivo measures of bite force have an advantage over theoretical models that tend to underestimate bite force due to model uncertainties such as muscle recruitment levels or true muscle stress values (Curtis et al., 2010; Gröning et al., 2013). Models, on the other hand can provide a direct link between shape variation and mechanical stress for a given loading regime allowing one to better understand the relationships between form and function. The shape associated with high absolute bite force is, as predicted, similar to that associated with the large temporalis cross sectional areas. Given that this is the largest jaw closer muscle in shrews (Gasc, 1963; Dötsch, 1986; Table 1) this is not surprising. Yet, shape variation associated with high absolute bite force is not closely related with shape associated with larger specimens suggesting that the allometric component in driving functional variation is small. The shape associated with the allometric component is more similar to that represented by the second overall shape axis.

When considering the shape associated with bite force scaled to centroid size, results are less clear. Although the temporal and frontal zones and the upper part of the rostrum also vary in relation to scaled bite force, the glenoid fossae appear to be more strongly affected. Moreover, this pattern is associated with the shape described by the first principal component axis describing overall shape variation in the dataset suggesting that the principal axis of shape variation is aligned with variation describing differences in relative bite force. This axis is not related to specimen size or population, but rather shows a high interindividual variability suggesting that subtle variations among individuals are captured by the first shape axis. Yet, this shape variation appears to be associated with relative differences in bite force and is reflected in variation in shape of the glenoid fossa. This may be reflecting the way, the reaction forces act across the jaw joint in individuals with different relative bite forces. Given the complexity of the jaw joint in shrews (Fearnhead et al., 1954) this needs to be explored in detail using detailed biomechanical models of the jaw joint.

When comparing island with continental specimens, our results highlight that the continental mean shape is similar to that represented by individuals with high bite force, high relative bite force, and large muscular PCSAs. Conversely, the mean shape of our island individuals is more similar to the shapes associated with low bite forces and low muscular cross sectional areas. This confirms earlier results suggesting that lower bite forces are present in insular populations of both *C. russula* and the closely related *C. suaveolens* on

the French Atlantic islands (Cornette et al., 2012, 2013). These differences are possibly related to differences in prey availability on islands (Young et al., 2009). Indeed, it is known that both the diversity and abundance of prey decreases with island size (Dayan and Simberloff, 1998). Alternatively, the differences in shape and bite force may be due to a relaxed selection on bite force due to a reduced competition on islands. These hypotheses remain to be tested and confirmed with larger sample sizes and for different islands. Moreover, the observed differences in skull shape may also be the results of founder effects or drift as is common in small island populations.

In summary, our results highlight how cranial shape variation is closely associated with variation in functional parameters in *C. russula*. Moreover, our methods highlight ways to explore shape variation associated with specific functional or anatomical parameters that, when coupled to 3D-geometric morphometric techniques and biomechanical models may allow for functional inferences in archaeological or fossil material.

ACKNOWLEDGMENTS

The authors want to thank Céline Houssin, Sibyle Moulin, Christian and Françoise Nantet, and Anne Claire Fabre for their help during this study. The authors also like to thank two anonymous reviewers and the editor for constructive and helpful comments on a previous version of the article that greatly helped improve it.

LIETERATURE CITED

Aguirre LF, Herrel A, Van Damme R, Matthysen E. 2002. Ecomorphological analysis of trophic niche partitioning in a tropical savannah bat community. Proc R Soc London B 269: 1271–1278.

Aguirre LF, Herrel A, Van Damme R, Mathyssen E. 2003. The implications of food hardness for diet in bats. Funct Ecol 17: 201–212.

Anderson R, McBrayer LD, Herrel A. 2008. Bite force in vertebrates: opportunities and caveats for use of a nonpareil whole-animal performance measure. Biol J Linn Soc 93:709–720.

Baylac M. 2012. Rmorph: A R Geometric and Multivariate Morphometrics Library. Available from the author: baylac@mnhn.fr. Accessed November 5, 2014.

Bookstein FL. 1997. Landmark methods for forms without landmarks: Morphometrics of group differences in outline shape. Med Image Anal 1:225–243.

Bookstein FL, Green WDK. 2002. Users Manual, EWSH3.19. Available at: http://brainmap.stat.washington.edu/edgewarp/. Accessed November 5, 2014.

Chazeau C, Marchal J, Hackert R, Perret M, Herrel A. 2013. Proximate determinants of bite force capacity in the mouse lemur, *Microcebus murinus*. J Zool 290:42–48.

Churchfield S. 1990. The Natural History of Shrews. Ithaca, New-York: Comstock Publishing, Cornell University Press. p. 178.

Cornette R, Herrel A, Cosson J-F, Poitevin F, Baylac M. 2012. Rapid morpho-functional changes among insular populations of the greater white-toothed shrew. Biol J Linn Soc 107:322–331.

Cornette R, Baylac M, Souter T, Herrel A. 2013. Does shape covariation between the skull and the mandible have functional consequences? A 3D approach for a 3D problem. J Anat 223: 329–336.

Currey JD. 2002. Bones, Structure, and Mechanics. Princeton: Princeton University Press. 436 p.

Currey JD. 2003. The many adaptations of bone. J Biomech 36: 1487–1495.

Curtis N, Jones MEH, Lappin AK, O'Higgins P, Evans SE, Fagan MJ. 2010. Comparison between in vivo and theoretical bite performance: Using multi-body modelling to predict muscle and bite forces in a reptile skull. J Biomech 43:2804–2809.

Dayan T, Simberloff D. 1998. Size patterns among competitors: Ecological character displacement and character release in mammals, with special reference to island populations. Mamm Rev 28:99–124.

Dötsch, C. 1986. Mastication in the Musk Shrew, *Suncus murinus* (Mammalia, Soricidae). J Morphol 189:25–43.

Fearnhead RW, Shute CCD, Bellairs Ad'A. 1954. The temporomandibular joint of shrews. Proc Zool Soc London 125:795–806.

Gasc J-P. 1963. La musculature céphalique chez *Suncus* Ehr., *Crocidura* Wag., *Sylvisorex* Thom., *Myosorex* Gr. Mammalia 27:582–601.

Gröning F, Jones MEH, Curtis N, Herrel A, O'Higgins P, Evans SE, Fagan MJ. 2013. The importance of accurate muscle modelling for biomechanical analyses: A case study with a lizard skull. J R Soc Interface 10:20130216.

Gunz P, Mitteroecker P. 2013. Semilandmarks: A method for quantifying curves and surfaces. Hystrix 24:103–109.

Gunz P, Mitteroecker P, Bookstein FL. 2005. Semi-landmarks in three dimensions. In: Slice D, editor. In Modern Morphometrics in Physical Anthropology. New York: Kluwer Academic/Plenum Publishers. p. 383.

Hanken J, Hall BK. 1993. The Skull, Vol. 3. Chicago, IL: The University of Chicago Press.

Hannam AG, Wood WW. 1989 Relationships between the size and spatial morphology of human masseter and medial pterygoid muscles, the craniofacial skeleton, and jaw biomechanics. Am J Phys Anthropol 80:429–445.

Herrel A, Holanova V. 2008. Cranial morphology and bite force in *Chamaeleolis* lizards—Adaptations to molluscivory? Zoology 111:467–475.

Herrel A, Spithoven L, Van Damme R, De Vree F. 1999. Sexual dimorphism of head size in *Gallotia galloti*; testing the niche divergence hypothesis by functional analyses. Funct Ecol 13: 289–297.

Herrel A, De Grauw E, Lemos-Espinal JA. 2001. Head shape and bite performance in xenosaurid lizards. J Exp Zool 290: 101–107.

Herrel A, Podos J, Huber SK, Hendry AP. 2005. Evolution of bite force in Darwin's finches: A key role for head width. J Evol Biol 18:669–675.

Herrel A, De Smet A, Aguirre LF, Aerts P. 2008. Morphological and mechanical determinants of bite force in bats: Do muscles matter? J Exp Biol 211:86–91.

Herring SW, Rafferty KL, Liu ZJ, Marshall CD. 2001. Jaw muscles and the skull in mammals: The biomechanics of mastication. Comp Biochem Physiol A 131:207–219.

Huber DR, Claes JM, Mallefet J, Herrel A. 2009. Is extreme bite performance associated with extreme morphologies in sharks? Physiol Biochem Zool 82:20–28.

Loeb GE, Gans C. 1986. Electromyography for Experimentalists. Chicago, IL: The University of Chicago Press. p. 373.

Mavropoulos A, Bresin A, Kiliaridis S. 2004. Morphometric analysis of the mandible in growing rats with different masticatory functional demands: Adaptation to an upper posterior bite block. Eur J Oral Sci 112:259–266.

Mendez J, Keys A. 1960. Density and composition of mammalian muscle. Metabolism 9:184–188.

Monteiro LR. 1999. Multivariate regression models and geometric morphometrics: The search for causal factors in the analysis of shape. Syst Biol 48:192–199.

Nogueira MR, Peracchi AL, Monteiro LR. 2009. Morphological correlates of bite force and diet in the skull and mandible of phyllostomid bats. Funct Ecol 23:715–723.

Paradis E, Claude J, Strimmer K. 2004. APE: analyses of phylogenetics and evolution in R language. Bioinformatics 20: 289–290.

R Development Core Team. 2013. R: A language and environment for statistical computing. Vienna, Austria: R Foundation for Statistical Computing. Available at: http://www.R-project.org.

Raadsheer MC, Van Eijden TMGJ, Van Ginkel FC, Prahl-Andersen B. 1999. Contribution of jaw muscle size and craniofacial morphology to human bite force magnitude. J Dent Res 78:31–42.

Rohlf FJ, Slice DE. 1990. Extensions of the Procrustes method for the optimal superimposition of landmarks. Syst Biol 39: 40–59.

Ross CF, Eckhardt A, Herrel A, Hylander WL, Metzger KA, Schaerlaeken V, Washington RL, Williams SH. 2007. Modulation of intra-oral processing in mammals and lepidosaurs. Integr Comp Biol 47:118–136.

Ross CF, Baden, AL, Georgi J, Herrel A, Metzger KA, Reed DA, Schaerlaeken V, Wolff MS. 2010. Chewing variation in lepidosaurs and primates. J Exp Biol 213:572–584.

Sharir A, Stern T, Rot C, Shahar R, Zelzer E. 2011. Muscle force regulates bone shaping for optimal load-bearing capacity during embryogenesis. Development 138:3247–3259.

Slizewski A, Schönau E, Shaw C, Harvati K. 2013. Muscle area estimation from cortical bone. Anat Rec 296:1695–1707.

Turnbull WD. 1970. Mammalian masticatory apparatus. Fieldiana: Geol 18:149–356.

Van Daele PAAG, Herrel A, Adriaens D. 2009. Biting performance in teeth-digging african mole-rats (*Fukomys*, Bathyergidae, Rodentia). Physiol Biochem Zool 82:40–50.

Wake DB, Roth G. 1989. Complex organismal functions: Integration and evolution in vertebrates. New York: Wiley & Sons Wiley.

Weijs WA, Hillen B. 1986. Correlations between the cross-sectional area of the jaw muscles and craniofacial size and shape. Am J Phys Anthropol 70:423–431.

Wiley DF, Amenta N, Alcantara DA, Ghosh D, Kil YJ, Delson E, Harcourt-Smith W, Rohlf FJ, St. John K, Hamann B, Motani R, Frost S, Rosenberger AL, Tallman L, Disotell T, O'Neill R. 2005. Evolutionary morphing. In: Proceedings of IEEE Visualization 2005 (VIS'05), October 23–28, 2005. Minneapolis, MN.

Wolff J. 1892. Das Gesetz der Transformation der Knochen. Berlin: August Hirschwald Verlag.

Young RL, Badyaev AV. 2010. Developmental plasticity links local adaptation and evolutionary diversification in foraging morphology. J Exp Zool B 314:434–444.

Young RL, Sweeney MJ, Badyaev AV. 2009. Morphological diversity and ecological similarity: Versatility of muscular and skeletal morphologies enables ecological convergence in shrews. Funct Ecol 24:556–565.